Biol Blood Marrow Transplant 25 (2019) 2045–2053

Biology of Blood and Marrow Transplantation

journal homepage: www.bbmt.org

Use of Multivariate Immune Reconstitution Patterns to Describe Immune Reconstitution after Allogeneic Stem Cell Transplantation in Children

Karin Mellgren[1,*], Andreas F.M. Nierop[2], Jonas Abrahamsson[1]

[1] *Department of Pediatrics, Institute of Clinical Sciences, Sahlgrenska Academy at University of Gothenburg, Gothenburg, Sweden*
[2] *Muvara bv, Multivariate Analysis of Research Data, Leiderdorp, The Netherlands*

Article history:
Received 22 September 2018
Accepted 19 June 2019

Keywords:
Stem cell transplantation
Immune reconstitution
Multivariate analysis

A B S T R A C T

Immune reconstitution after hematopoietic stem cell transplantation (HSCT) is a complex process. Impacts of the reconstitution of different immune cells over time are complex and difficult to understand. New mathematical models are needed to better understand this process. In this study, we used principal component analysis to better analyze the process of immune reconstitution after HSCT. Forty-six consecutive patients receiving HSCT for malignant and nonmalignant disorders were included in the study. All patients were followed for at least 24 months after transplantation with regular blood sampling for analysis of lymphocyte subset numbers and function. Exponentially transformed lymphocyte subset counts and lymphocyte functional markers were analyzed to identify major trends in the reconstitution process. Using our multivariate model for mapping immune reconstitution after HSCT, we showed that dysfunctional reconstitution patterns precede severe complications, such as chronic graft-versus-host disease, relapse, and death.

© 2019 American Society for Transplantation and Cellular Therapy. Published by Elsevier Inc.

INTRODUCTION

The speed and quality of immune reconstitution are important factors in clinical outcomes after hematopoietic stem cell transplantation (HSCT). Immune reconstitution in this setting is a stepwise process in which the innate immune system starts to recover before the adaptive system [1]. In particular, the timing of T and B lymphocyte reconstitution has been associated with increased risks of post-transplantation opportunistic infections and transplantation-related mortality in various studies [2–7]. Furthermore, the timing of reconstitution of the various lymphocyte subtypes and their functions are related to clinical outcomes after transplantation, in particular, the occurrence of graft-versus-host disease (GVHD), relapse of malignant disease, and infectious complications. The reconstitution of adaptive immunity after HSCT can be influenced by several factors, including recipient age, donor (related/unrelated, HLA-matched/mismatched), conditioning (myeloablative/reduced intensity, inclusion of radiation therapy), ex vivo or in vivo T cell depletion of the graft, infections and their treatment, type of GVHD prophylaxis, and occurrence and treatment of GVHD [8].

In clinical practice, there is a clear need for simple and reliable markers of immune reconstitution to allow clinicians to identify patients at risk of transplantation-related complications. Various single markers have been proposed to be predictive of outcome. For example, the recovery pace of absolute lymphocyte count has been used as a proxy for the overall recovery of immune function [9]. Slow recovery of specific T cells reportedly has a significant impact on patient survival [10–12]. High levels of $CD4^+$ T cells and natural killer (NK) cells are associated with protection against cytomegalovirus reactivation [13]. Patients with low $CD4^+$ T cell counts on day 35 post-HSCT are at greater risk of dying of infection [6]. Moreover, the speed of reconstitution of cytotoxic $CD8^+$ T cells has been correlated with survival [14]. In addition, B cell recovery reportedly predicts the risk of infections after HSCT [7]. A study focusing on the B cell compartment after HSCT showed that this is not functionally mature for years after HSCT [15]. Particularly, the development of IgM^+CD27^+ B cells, a cell type implicated in protection against infections with encapsulated bacteria, is delayed for years after HSCT. Previous studies on predictive biomarkers for events have focused mainly on NK and T cells [16], although B cells may play a role in the occurrence of relapse in adult patients [17]. Although B cell numbers are normal within a year after transplantation, they still show diminished in vitro responses to polyclonal activators 2 years after transplantation [15].

Financial disclosure: See Acknowledgments on page 2052.

* Correspondence and reprint requests: Karin Mellgren, MD, PhD, Department of Pediatric Hematology and Oncology, Queen Silvia's Hospital for Children, Rondvägen 10, 41685 Gothenburg, Sweden.
E-mail address: karin.mellgren@vgregion.se (K. Mellgren).

https://doi.org/10.1016/j.bbmt.2019.06.018
1083-8791/© 2019 American Society for Transplantation and Cellular Therapy. Published by Elsevier Inc.

The problem with using a single marker for predicting outcomes is that studies do not take into account the heterogeneity of patients in terms of such factors as conditioning, graft type, and composition and type of donor, which may influence the results. Furthermore, the normalization of B and T cell numbers does not necessarily indicate reconstitution of their function [16]. Therefore, there is a need for better understanding of the correlation between immune system dysfunction after HSCT and the occurrence of complications of treatment. A more reliable model of immune reconstitution will enable better identification of patients at risk for complications, which may help guide treatment with available immune therapies.

Models describing immune function have been published previously. Koenig et al [18] constructed a 3-component multivariate model with a reference domain of ellipsoidal shape based on normal leukocyte subtype values from healthy children and adolescents. This model was used to classify pediatric patients as having high or low risk for a post-transplantation event according to their immune reconstitution. Ek et al [19] used a principal component analysis (PCA) model to predict immune reconstitution after treatment for leukemia, and Hunecke et al [20] used a continuous regression model to reflect normal immune maturation in healthy young children.

In this study, we collected data on disease, graft type, conditioning, and donor, as well as immunological data on lymphocyte subset numbers and function, and elaborated a statistical model permitting the identification of different immune reconstitution patterns for these patients. Our results show that dysfunctional reconstitution patterns are associated with, and even precede, complications such as relapse and death.

METHODS

Patients

The study cohort comprised 46 consecutive patients (26 boys and 20 girls) who underwent transplantation at Queen Silvia's Hospital for Children and Adolescents in Gothenburg, Sweden for malignant (34 patients) and nonmalignant (12 patients) disorders. These patients underwent a total of 50 transplants; 4 patients underwent 2 transplantations. Informed consent was obtained from guardians and, when appropriate, from the children. Studies were conducted in accordance with the Declaration of Helsinki and approved by the Ethical Committee in Gothenburg.

All patients were followed up for at least 48 months after transplantation with regular blood sampling for analysis of lymphocyte subset numbers and function. Peripheral blood was collected during the week before conditioning began and at 3, 6, 9, 12, 18, and 24 months after transplantation. The clinical characteristics of the 46 patients are summarized in Table 1.

The conditioning regimen was myeloablative in 43 transplantations and nonmyeloablative in 6. One patient with severe combined immunodeficiency received no conditioning, with only antithymocyte globulin (ATG) before transplantation. Conditioning was busulfan-based in 23 transplantations, was total body irradiation-based in 24 transplantations, and involved other treatments in the remaining 3 transplantations (Table 1).

GVHD prophylaxis was given with cyclosporin A or tacrolimus (target trough levels 150 to 220 ng/mL and 12 to 15 ng/mL, respectively) and maintained for a period of 3 to 6 months (shorter times for malignant diseases with matched family donors) before tapering. In all cases where an unrelated donor was used, as well as in most cases of HSCT for benign disorders, a short course of methotrexate (10 mg/m^2 on days +1, +3, and +6) was added.

All patients but 1 with hematologic malignancy were in complete morphologic remission at the time of HSCT. The patient who was not in remission at the time of HSCT underwent transplantation for relapse of acute lymphoblastic leukemia and had another relapse at day 21 post-transplantation.

Flow Cytometry of Peripheral Blood Lymphocytes

Flow cytometry was performed on a FACScan instrument (BD Biosciences, San Jose, CA). The monoclonal antibodies used were anti-CD3, -CD4, -CD8, -CD19, -CD45RA, and -CD45RO (BD Biosciences). The absolute number for each lymphocyte subset was calculated by multiplying the percentage of marker-positive cells by the absolute lymphocyte count determined using a hematologic cell counter (Sysmex-K1000 or K4500; TOA Medical Electronics, Kobe, Japan) and expressed as the number of positive cells $\times$ 10^9/L. The following subsets of B and T lymphocytes were explored: CD19$^+$ cells (B cells), CD3$^+$CD4$^+$CD45RA$^+$ naive T helper cells (T4N), CD3$^+$CD4$^+$CD45RO$^+$ memory T helper cells (T4M), CD3$^+$CD8$^+$CD45RA$^+$ naive cytotoxic T cells (T8N), and CD3$^+$CD8$^+$CD45RO$^+$ memory cytotoxic T cells (T8M) (See Table 2).

Functional Analysis

Proliferation of mononuclear cells after mitogen stimulation was assessed after incubation with phytohemagglutinin (PHA; 10 mg/mL; Murex Biotech, Dartford, Kent, UK), concanavalin A (50 mg/mL; Sigma-Aldrich, St Louis, MO), or monoclonal anti-CD3 (125 ng/mL; Ortho Diagnostic Systems, Raritan, NJ). Proliferation was measured as incorporation of 3H-thymidine as described previously [21]. The results are expressed as a percentage in relation to that in healthy blood donors (obtained value/value from blood donor $\times$ 100).

The number of immunoglobulin-producing cells was measured by enzyme-linked immunospot assay after 6 days of incubation of lymphocytes with pokeweed mitogen (PWM) or Epstein-Barr virus (EBV). The produced immunoglobulins were linked to antigens in the incubation chamber and visualized by enzyme-conjugated antibodies against IgG, IgA, or IgM. A spot appears at the location of each immunoglobulin-producing cell, and the result is expressed as spots per million cells.

Serum immunoglobulin levels (IgG, IgA, and IgM) and subclasses of IgG (IgG1, IgG2, IgG3, and IgG4) were measured by radial immunodiffusion, and the results are expressed in g/L. IgE was measured using antibodies covalently bound to a specific, large surface (an ImmunoCAP) by fluorescence enzyme immunoassay, and the results are expressed as kU/L.

Quantification of T cell receptor rearrangement excision circles (TRECs) was performed after DNA extraction and PCR analysis. The results are expressed as number of TREC molecules/1,000,000 cells (See Table 2).

Statistical Analysis

Blood samples were drawn at 0, 3, 6, 12, 18, and 24 months after HSCT, resulting in a total of 276 measurements. For multivariate analysis, the 204 measurements with fewer than 12 missing values were selected, and 72 measurements with 12 or more missing values were excluded. Furthermore, all data obtained after the occurrence of an event—defined as death, graft rejection, or relapse of malignant disease—were omitted, leaving a total of 195 measurements of 24 immune variables.

Transplantation characteristics included malignant/benign disease, total body irradiation-based conditioning or other, reduced-intensity conditioning or myeloablative conditioning, matched family donor or matched unrelated donor, and bone marrow, peripheral blood, or cord blood stem cell source.

Outcome parameters included presence or absence of chronic GVHD (cGVHD); presence or absence of graft rejection; relapse of malignant disease after HSCT; presence of an event, defined as graft rejection, relapse, or transplantation-related mortality; and alive or dead at last follow-up.

PCA

Using the measured immune variables, an unsupervised immune reconstitution model for patients without events was computed with a PCA performed on 24 exponentially transformed immune variables. The data were preprocessed in 3 steps: First, PWM and EBV variables were adjusted by setting all negative values to 0. Second, all immune were transformed by fitting the measurement values, x, of the patients with an exponential cumulative distribution function with 1 parameter, expCDF(x, mu)=1 $-$ e$^{-x/mu}$. If the minimum value of a variable was tied, all repeated minimum values were omitted, leaving only 1 minimum value for use in the fitting procedure. Third, the model was constructed so that each variable was mathematically transformed to have the same chance of influencing the PCA solution. Thus, in the initial data handling, the variables were transformed to give each variable a unit variance, all exponentially transformed variables were mean-centered and standardized to unit variance, and missing data were set to 0. The PCA component scores were scaled to unit variance.

Reducing the Number of Immune Variables in the Immune Reconstitution Model

We aimed to approximate the first 2 components of the PCA model for patients without events, which included all 24 immune variables, with fewer variables using a modification of reflected discriminant analysis (RefDA). This model can be described as a mixture between discriminant analysis (also called canonical variate analysis) and PCA [21,22]. The orthonormal group mirror space in RefDA [22] was replaced by the orthonormal principal component (PC) 1-2(24vars) mirror space of the first 2 components of the PCA with 24 variables. This modification of RefDA is referred to as reflected component analysis (RefCA) and includes a more general mirror space. In a stepwise forward approach, the number of selected variables was increased by adding the variable that most increased the geometric mean of the reflected variances. In general, as more variables are selected, the squared canonical correlations of the reflected components with the first 2 components of the PCA increase, giving an impression of how well the PCA components are approximated by the reflected components. In contrast, the percentage of explained variance of the selected variables decreases, giving an impression

Table 1
Patient Characteristics

Patient	Age (Years)	Disease	Conditioning	Donor	Source	TCD	GVHD Prophylaxis	aGVHD	cGVHD	Rejection	Relapse	Outcome	Follow-Up, mo
196	18.5	CML, CP2	BU/FLU/ATG (RIC)	MUD	PBSC	No	FK/MTX	No	No	No	No	Alive	63
221	.4	Osteopetrosis	BU/CY/ATG	MUD	PBSC	No	CYA/MTX	No	No	No	N/A	Dead, TRM	2
222-1	.7	SCID	BU/FLU/ATG (RIC)	MMFD	PBSC	Yes	CYA	No	No	Yes	N/A	Alive	98
222-2	.9	SCID	ATG (No)	MUD	PBSC	Yes	CYA/MTX	Grade II	No	No	N/A	Alive	96
225	5.5	ALL, CR3	TBI/CY	MFD	BM	No	CYA	Grade III	Extensive	No	No	Alive	96
226	.7	Osteopetrosis	BU/CY/ATG	MFD	PBSC	No	CYA	No	No	No	N/A	Dead, TRM	9
230	2.1	ALL, CR1	BU/CY/ATG	MUD	BM	No	FK/MTX	No	No	No	No	Alive	92
231	8.0	AML, CR1	BU/CY	MFD	BM	No	FK	No	No	No	Yes	Dead	8
236	7.0	ALL, CR2	TBI/CY/ATG	MUD	PBSC	No	CYA/MTX	Grade I	Extensive	No	No	Alive	85
238	13.3	ALL, CR2	TBI/CY	MFD	BM	No	FK	No	No	No	No	Alive	82
239	16.9	ALL, CR1	TBI/CY	MFD	BM	No	FK	Grade II	Extensive	No	No	Dead, TRM	28
241	1.1	AML, CR2	BU/CY/ATG	MUD	BM	No	FK/MTX	No	No	No	No	Alive	80
245	1.6	AML, CR1	BU/CY/ATG	MUD	BM	No	FK/MTX	No	No	No	No	Alive	77
246	4.6	ALL, Ph^+, CR1	TBI/CY/ATG	MUD	BM	No	FK/MTX	No	Limited	No	Yes	Alive	75
249	6.6	ALL, CR2	TBI/CY	MFD	BM	No	FK	Grade I	Limited	No	No	Alive	63
251	.9	WAS	BU/CY/ATG	MUD	Cord	No	FK/MTX	No	Extensive	No	N/A	Alive	72
253	7.7	ALL, CR2	TBI/CY	MUD	PBSC	No	FK/MTX	No	No	No	No	Alive	72
256	1.5	AML, CR1	BU/CY	MFD	PBSC	No	FK/MTX	No	No	No	No	Alive	70
257	1.6	AML, CR2	BU/CY	MFD	PBSC	No	FK/MTX	No	Extensive	No	Yes	Dead	22
258	11.9	SAA	CY/ATG (RIC)	MFD	BM	No	FK/MTX	No	No	No	N/A	Alive	68
259-1	1.1	CML, CP1	BU/CY	MFD	PBSC	No	FK/MTX	No	No	no	Yes	Alive	67
259-2	1.9	CML, CP2	TBI/VP/CY	MUD	PBSC	No	FK/MTX	No	Extensive	No	No	Alive	58
260-1	4.9	CGD	BU/CY/ATG	MUD	PBSC	No	FK/MTX	No	No	Yes	N/A	Alive	66
260-2	5.3	CGD	FLU/MEL/C1H	MUD	PBSC	No	FK	No	No	No	N/A	Alive	61
261	.9	Hyper-IGM syndrome	BU/CY	MUD	BM	No	FK/MTX	No	No	No	N/A	Alive	65
263	10.4	ALL, CR2	TBI/CY/ATG	MUD	BM	No	FK/MTX	Grade I	No	No	No	Alive	61
264	11.0	CML, CP1	BU/CY	MFD	BM	No	FK/MTX	Grade II	No	No	Yes	Alive	60
265	1.7	JMML	BU/CY/MEL/ATG	MUD	BM	No	FK/MTX	Grade I	No	No	No	Alive	58
266	2.7	Osteopetrosis	BU/CY/ATG	MUD	BM	No	FK/MTX	No	No	No	N/A	Alive	56
267	14.8	ALL, Ph^+, CR1	TBI/CY	MFD	BM	No	FK/MTX	Grade III	Limited	No	No	Alive	56
268	13.4	ALL, CR3	TBI/CY	MFD	PBSC	No	FK/MTX	No	Limited	No	Yes	Dead	16
270	9.2	CID	TBI/ FLU (RIC)	MFD	BM	No	FK/MMF	Grade I	No	Yes	N/A	Alive	54
271	4.4	ALL, CR1	TBI/CY	MFD	BM	No	FK	Grade IV	No	No	No	Dead, TRM	5
273	4.0	NHL, CR2	TBI/CY	MFD	BM	No	FK	Grade I	Limited	No	Yes	Dead	7
274	6.7	ALL, CR2	TBI/CY	MUD	BM	No	FK/MTX	No	No	No	Yes	Dead	29
275	3.0	ALL, CR2	TBI/CY/ATG	MUD	BM	No	FK/MTX	No	No	No	Yes	Dead	2
276	14.3	ALL, CR1	TBI/CY/ATG	MUD	PBSC	No	FK/MTX	No	Limited	No	No	Alive	48
277	13.7	CGD	BU/CY/C1H	MUD	PBSC	No	FK/MTX	Grade I	Limited	No	N/A	Alive	47
278-1	12.9	Thalassemia	BU/CY/ATG	MFD	PBSC	No	FK/MMF	No	No	Yes	N/A	Alive	46

(*continued*)

Table 1 (*Continued*)

Patient	Age (Years)	Disease	Conditioning	Donor	Source	TCD	GVHD Prophylaxis	aGVHD	cGVHD	Rejection	Relapse	Outcome	Follow-Up, mo
278-2	13.7	Thalassemia	BU/CY/FLU/C1H	MUD	PBSC	No	CYA/ Solumedrol	No	No	No	N/A	Alive	36
279	10.0	ALL, CR2	TBI/VP/CY/ATG	MUD	BM	No	FK/MTX	Grade I	Limited	No	No	Alive	45
280	15.4	ALL, CR2	TBI/VP/CY	MFD	BM	No	FK/MTX	No	Limited	No	No	Alive	44
281	15.4	CML, CP2	TBI/CY	MFD	BM	No	FK	No	Limited	No	Yes	Alive	43
282	10.6	ALL, CR1	TBI/VP/CY/ATG	MFD	BM	No	FK/MTX	No	No	No	Yes	Alive	41
283	18.1	NHL, CR2	TBI/VP/CY	MFD	BM	No	FK	No	No	No	No	Alive	41
284	2.5	XLP	BU/CY	MFD	BM	No	FK/MTX	No	No	No	N/A	Dead, TRM	4
285	1.5	AML, CR1	BU/CY/ATG	MUD	BM	No	FK/MTX	No	No	No	No	Alive	38
286	17.9	NHL, CR2	TBI/CY	MFD	BM	No	FK/MTX	No	Extensive	No	No	Alive	37
288	15.6	ALL, CR1	BU/VP/CY/ATG	MUD	PBSC	No	FK/MTX	Grade I	NA	No	No	Dead, TRM	6
290	3.6	ALL, CR2	TBI/VP/CY	MFD	BM	No	FK/MTX	No	No	No	No	Alive	33

TCD indicates T cell depletion; CML, chronic myelogenous leukemia; SCID, severe combined immunodeficiency; ALL, acute lymphoblastic leukemia; WAS, Wiskott-Aldrich syndrome; SAA, severe aplastic anemia; JMML, juvenile myelomonocytic leukemia; CID, combined immunodeficiency; NHL, non-Hodgkin lymphoma; CGD, chronic granulomatous disease; XLP, X-linked lymphoproliferative disease; Ph^+, Philadelphia chromosome-positive; CR, complete remission; CP, chronic phase; BU, busulfan; FLU, fludarabine; RIC, reduced-intensity conditioning; TBI, total body irradiation; CY, cyclophosphamide; VP, etoposide; MEL, melphalan; C1H, MabCampath; MUD, matched unrelated donor; MFD, matched family donor; MMFD, mismatched family donor (haploidentical); FK, tacrolimus; CYA, cyclosporine A; MTX, methotrexate; MMF, mycophenolate mofetil; TRM, transplantation-related mortality.

of how well the reflected components are supported by all selected variables. In general, as more variables are selected, the geometric mean of the reflected variances will first increase toward a maximum value and then decrease, because the reflected variance criterion is an integrated measure of squared canonical correlations and explained variance.

Function-Number transformation

To facilitate a more detailed clinical interpretation of the PCA model concerning B and T lymphocyte responses to stimulation (function of cells) and lymphocyte subset numbers (number of cells), the principal components PC1 and PC2 and the corresponding loadings were rotated 45 degrees counterclockwise, so that "function of cells" = $(PC1 - PC2)/2^{1/2}$ and "number of cells" = $(PC1 + PC2)/2^{1/2}$. Likewise, the reflected components ReflComp1 and ReflComp2, approximating the PCA components with fewer variables, were transformed as "function of cells" = $(ReflComp1 - ReflComp2)/2^{1/2}$ and "number of cells" = $(ReflComp1 + ReflComp2)/2^{1/2}$.

Group centroid separation was tested in 4 different directions: PC1, PC2, "number of cells," and "function of cells," by performing *t* tests, assuming that the 2 samples have normal distributions with unknown and unequal variances. We considered statistically significant separation as differences with $P < .05$ and highly statistically significant differences as those with $P < .001$.

RESULTS

Patient Data and Clinical Follow-Up

Fifty transplantations were performed in the 46 patients. Four patients underwent a second transplantation with a new donor, 3 after graft rejection and 1 with chronic myelogenous leukemia who relapsed with blast crisis shortly after the first transplantation. For these patients, follow-up data are reported from the second transplantation only. The median duration of follow-up was 91.2 months (range, 1.6 to 139.3 months).

Fifteen patients developed acute GVHD (aGVHD), including 12 with grade I-II and 3 with grade III-IV, and 17 developed cGVHD, including 9 with limited disease and 8 with extensive disease. One patient rejected the graft after 60 days and experienced an autologous recovery of marrow function. Ten of the 34 patients with malignant disease relapsed after transplantation. The median time to relapse was 9.4 months (range, 1.1 to 55.0 months), and only 4 patients relapsed before 6 months. Seven of the 10 patients died after relapse. In addition, 7 patients died from transplantation-related complications. The median survival time after HSCT in these patients was 16.8 months (range, 4.8 to 66.9 months). An event—defined as relapse of malignant disease, rejection of graft, or death from a transplantation-related cause—occurred in 18 of the 46 patients. Estimated event-free survival and overall survival for the whole cohort at 5 years were 63.0 ± 7.1% and 71.7 ± 6.6%, respectively. The median time to an event was 8.3 months (range, 1.1 to 97.8 months).

Immune Variables

Mean values of all 24 immune variables for different subgroups of patients within each time point, including pairwise comparisons between subgroups, are presented in Supplementary Tables I to IV.

Exponential Transformation of Immune Variables

All immune variables with measurement values, *x*, were transformed with the exponential function $F_{\text{transformed}} = 1 - e^{-x/mu}$. The fitted mu values for the 24 immune variables to be substituted into this formula were as follows: IgG, 8.8337; IgA, .95278; IgM, .99438; IgE, 37.54; IgG1, 4.9276; IgG2, 1.9406; IgG3, .62464; IgG4, .2117; B cells, .47947; T4N cells, .31103; T4M cells, .25756; T8N cells, .48477; T8M cells, .47894; TRECs, 31.059; EBV-IgM, 153.65; PWM-IgM, 23.605; EBV-IgG, 27.749; PWM-IgG, 13.376; EBV-IgA, 44.822; PWM-IgA, 17.109; unstimulated, 216.15; PHA-stimulated, 64.995; concanavalin A-stimulated, 68.132; and CD3-stimulated,

Table 2
Immune Variables Included in the Study

Short Name	Specification	Abbreviation	Explanation	Unit
Cell number	Number of B lymphocytes	B cells	$CD19^+$ cells	Number of cells $\times 10^9$/L
Cell number	Number of T lymphocyte subsets	T4N	$CD3^+4^+45RA^+$ naive T helper cells	Number of cells $\times 10^9$/L
		T4M	$CD3^+4^+45RO^+$ memory T helper cells	
		T8N	$CD3^+8^+45RA^+$ naive cytotoxic T cells	
		T8M	$CD3^+8^+45RO^+$ memory cytotoxic T cells	
Immunoglobulin levels	Immunoglobulin levels	IgG, IgA, IgM, IgE	Levels of IgG, IgA, IgM, IgE,	kU/L (IgE) or g/L
	Immunoglobulin G subsets	IgG_1, IgG_2, IgG_3, IgG_4,	Levels of IgG_1, IgG_2, IgG_3, IgG_4,	
T-cell receptor excision circuits	T-cell Receptor Excision Circuits	TREC	Number of TREC molecules	Number of TRECs per 1,000,000 cells.
Cell function	B-lymphocyte response to stimulation	EBVIgG	IgG,A,M production after stimulation with EBV	% in relation to healthy blood donors
		EBVIgA		
		EBVIgM		
		PWMIgG	IgG,A,M production after stimulation with PWM	
		PWMIgA		
		PWMIgM		
Cell function	T-lymphocyte response to stimulation	Unstim	Incorporation of radioactive thymidine into DNA without stimulation	% in relation to healthy blood donors
		PHAstim	Incorporation of radioactive thymidine into DNA after stimulation with PHA, ConA, or CD3	
		ConAstim		

ConA indicates concanavalin A.

54.245. As an example, for IgG, the corresponding formula of the exponential transformation is $IgG_{transformed} = 1 - e^{-(IgG\ value)/8.8337}$.

Multivariate Immune Reconstitution Model

In Figure 1, the results of PCA on the 24 exponentially transformed immune variables (PCA24vars) are presented graphically in a combined plot with scores and vectors showing the correlations of these scores with the immune variables and background characteristics. Some background characteristics have such low correlations with the PCA scores that they are not shown in the plot. As indicated in Figure 1 by "number of cells" and "function," both absolute numbers of lymphocyte subsets and lymphocyte function are important for the model of total immune reconstitution.

We also studied whether the first 2 components of the PCA24vars solution could be approximated with fewer variables and found that 7 variables were sufficient to give a good approximation: the numbers of T4N cells, T4M cells, and T8M cells; level of IgG1; T cell stimulation by PHA; and IgG and IgA production after stimulation of B cells by PWM (Figure 2, RefCA7vars).

Time Plots of Function and Number of Cells

To facilitate a more detailed clinical interpretation of the "function of cells" and "number of cells" in Figure 2, in Figure 3 we plotted the mean ± SEM reconstitution curves for different subgroups of patients vs. months post-HSCT. The numbers of lymphocyte subsets (number of cells), as well as B and T lymphocyte response to stimulation (function of cells), reached a nadir at 3 months after HSCT and increased over time thereafter (Figure 3A). As expected, patients with cGVHD had a slower reconstitution pattern than patients without cGVHD (Figure 3B). This difference was most pronounced at 12 months after transplantation ($P = .039$), and the differences in cell numbers as well as in cell function remained until 24 months after transplantation. As shown in Figure 3C, patients with malignant and benign disease showed similar reconstitution patterns. The reconstitution pattern in patients receiving a transplant from a family donor was largely similar to that in patients receiving transplants from a matched unrelated donor (Figure 3D).

The reconstitution pattern for patients receiving ATG before transplantation was very similar to that for matched unrelated donors and matched family donors, as shown in Figure 1 (phi coefficient comparing ATG with donor type, .93). In our study, all patients who underwent HSCT with an unrelated donor graft received ATG or MabCampath (alemtuzumab) as part of the conditioning regimen, whereas only 3 patients who received a graft from a family donor received ATG in conditioning (Table 1).

When analyzing patients undergoing HSCT for a malignant disease, we observed that those who developed a subsequent event (defined as relapse of malignant disease or transplantation-related mortality) had slower reconstitution patterns than those without an event (Figure 4). Patients with a subsequent event had lower numbers of lymphocyte subsets and reduced B and T lymphocyte responses to stimulation from 3 to 12 months after transplantation.

DISCUSSION

In this study of 46 pediatric HSCT recipients, we elaborated a PCA model describing immune reconstitution patterns in different groups of patients. The model takes into account the absolute numbers of different subsets of T and B cells, as well as of functional tests on B and T cells, at different time points in children after allogeneic HSCT. An important finding is that 7 of the variables were sufficient to

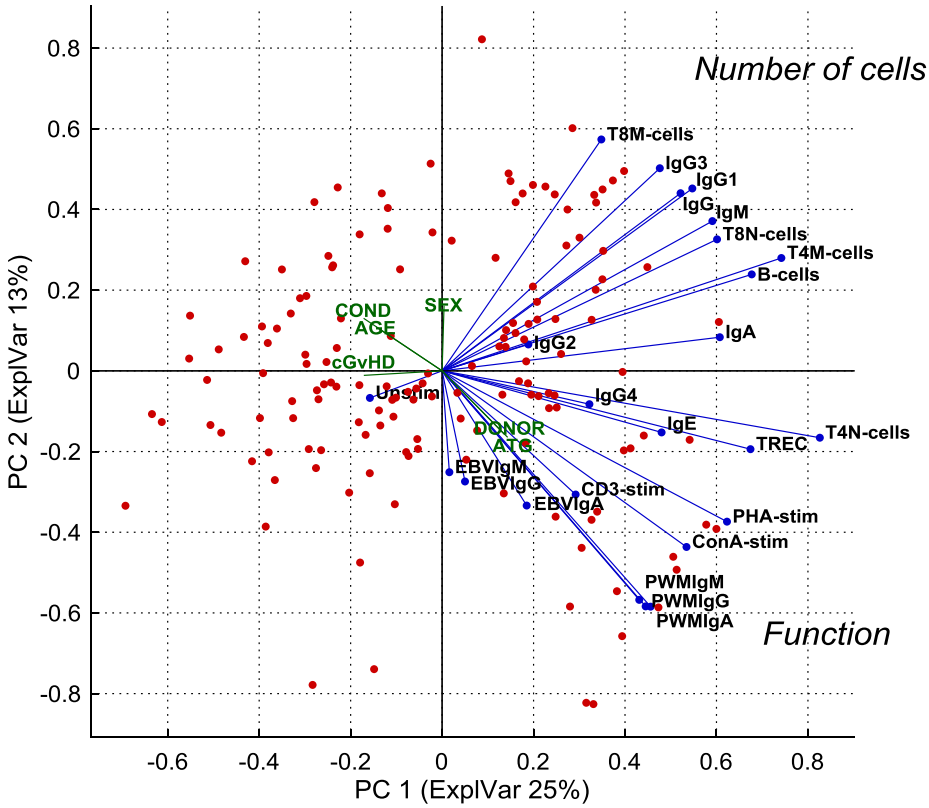

Figure 1. PCA24vars, the PCA model including all 24 immune variables for patients without events, defined as transplantation-related mortality, graft rejection, or relapse of malignant disease. The origin represents the mean score for all measurements (red dots) in the PCA and also can be interpreted as mean immune reconstitution at each measurement. The blue vectors represent the contribution of the individual variables to the PCA components. Thus, measurements to the right in the plot (positive score on PC1) have higher mean scores for the variables representing immune reconstitution. PC2 further separates measurements into those with higher number of cells (upper right quadrant, positive PC2 values) and higher levels of variables representing function (lower right quadrant, negative PC2 values). The green vectors show the correlation with background characteristics.

construct a reliable model: numbers of $CD3^+CD4^+CD45RA^+$ naive T helper cells, $CD3^+CD4^+CD45RO^+$ memory T helper cells, and $CD3^+CD8^+CD45RO^+$ memory cytotoxic T cells; IgG1 level; T cell stimulation by PHA; and IgG and IgA production after stimulation of B cells by PWM. Another important finding is that in the group of patients with malignant disease, the occurrence of relapse or transplantation-related death was characterized by a slower immune reconstitution pattern, as well as reduced T lymphocyte subset numbers and lymphocyte response to in vitro stimulation, which could be observed months before the event occurred.

The identification of immune biomarkers predictive of transplantation-related complications associated with immune reconstitution is of great interest for clinical practice. Such markers would allow clinicians to individualize immune suppression [16]. Several studies have investigated the predictive value of 1 or more lymphocyte subsets and their association with events [9–14], but all were limited by such factors as a small number of patients and heterogeneity in disease, conditioning regimen, graft type, and other transplantation characteristics. The process of immune reconstitution after HSCT is complex, with various interactions between different components of the immune system [16], and reconstitution of lymphocyte subsets, in both numbers and function, follows different timelines [17]. Therefore, the quality of the immune response is influenced by the quality of immune function of the different cell types, rather than by the absolute numbers of cells. Recent studies have emphasized the relationship between low T cell responses to mitogen stimulation early after transplantation and poor survival [23]. Other studies have highlighted the relationship between slow immune reconstitution, in particular low $CD4^+$ cell numbers early after HSCT, and viral infections [6].

The use of conventional statistical methods places difficult constraints on raw data, particularly in large datasets, in which problems with mass significance can easily occur. According to the American Statistical Association, "conducting multiple analyses of the data and reporting only those with certain *p* values renders the reported *p* values essentially unpredictable" [24]. Indeed, a multivariate model gives a more complete picture of the immune reconstitution pattern [18–20,25].

Using our model, we were able to comprehensively visualize immune reconstitution and to observe different reconstitution patterns in different situations. As expected, patients with cGVHD had a delayed reconstitution pattern compared with those without cGVHD, consistent with an earlier report of lymphocyte reconstitution in adult patients that used multivariate methods [17]. It has been suggested that differences in immune reconstitution of B and T cells might be present even before the onset of clinical symptoms of cGVHD [26]. Our study cohort was not large enough to allow us to test whether immune reconstitution can be used as a predictive marker for cGVHD, but we can confirm that immune reconstitution in terms of cell numbers and cell function is impaired in patients with cGVHD.

Recent studies have suggested that the host immune microenvironment before transplantation may have an impact on the occurrence of GVHD and relapse in patients with

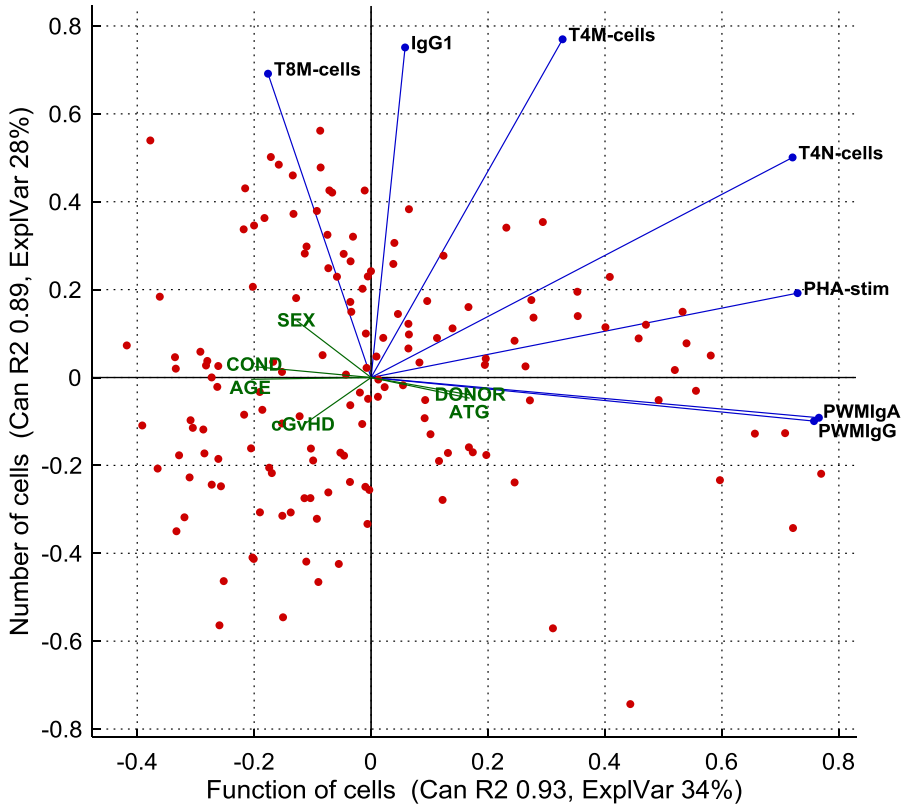

Figure 2. RefCA7vars. The 7 variables most important for the immune reconstitution model were computed using reflected component analysis, and the approximation is shown after a function-number transformation, rotating the reflected components 45 degrees counterclockwise. The squared canonical correlations of "function of cells" and "number of cells" with the planes of the first 2 components of PCA24vars in Figure 1 are .93 and .89, respectively. The origin represents the mean score for all measurements (red dots) in the PCA and also can be interpreted as mean immune reconstitution at each measurement. The blue vectors represent the contribution of the individual variables to the PCA components. Thus, measurements with higher scores on the *x*-axis have higher mean levels for the variables representing cell function, and those with higher scores on the *y*-axis have higher mean levels for variables representing cell numbers. The green vectors show the correlation with background characteristics.

malignant disease [17]. In our study, we observed a slight difference in lymphocyte numbers before transplantation in patients who subsequently developed cGVHD. Interestingly, we also observed reduced lymphocyte function in patients undergoing HSCT for a nonmalignant disease who subsequently died from a transplantation-related cause or developed graft rejection. These data could support the hypothesis that the host immune microenvironment before transplantation influences the immune reconstitution pattern and probability of an event; however, larger studies in a prospective setting are needed to confirm this hypothesis.

Our model shows a similar immune reconstitution pattern in patients undergoing HSCT for benign disease and those doing so for malignant disease. Studies performed in adult patients with malignant disease found no differences in lymphocyte sequential patterns according to disease or conditioning but did identify differences based on the type of HSCT, with a different reconstitution pattern in patients receiving a haploidentical graft [27]. Lymphocyte numbers and function were low even before the start of transplantation in patients with malignant disease, probably reflecting the effect of intensive pre-HSCT chemotherapy, as described previously [19]. In our study, immune patterns differed significantly before transplantation between patients receiving stem cells from a matched family donor and those receiving cells from a matched unrelated donor.

The role of ATG in conditioning regimens has been highlighted in recent studies in which the reconstitution rate was impaired after the use of ATG, influenced by ATG dose and type [28,29]. Slow reconstitution of $CD4^+$ T cells is reportedly associated with an increased risk of viral infection. [30]. In our study, all patients receiving stem cells from an unrelated donor received ATG as part of the conditioning regimen, as did 3 patients with benign disease receiving stem cells from a family donor. Accordingly, the different immune reconstitution patterns in patients receiving ATG and those receiving transplants from an unrelated donor overlapped, and thus the differences observed between patients receiving stem cells from a family donor and from a matched unrelated donor might be explained by the use of ATG in the conditioning regimen.

Another limitation of the present study is the lack of data on viral infections and its influence on immune reconstitution.

Interestingly, our model allowed us to observe a specific immune reconstitution pattern in the group of 34 patients who underwent HSCT for malignant disease, in which patients with subsequent relapse or death due to transplantation-related causes showed slower immune reconstitution, with smaller numbers of lymphocyte subsets and reduced B and T lymphocyte responses to stimulation, compared with patients without an event. Because the data were censored at the time of the event, this immune pattern does indeed indicate differences in cell function before event occurrence.

In this study, we reported a cohort of patients analyzed as a test set, and a validation set is needed to determine whether our model of immune reconstitution could function as a predictive tool. We have shown that our multivariate model for

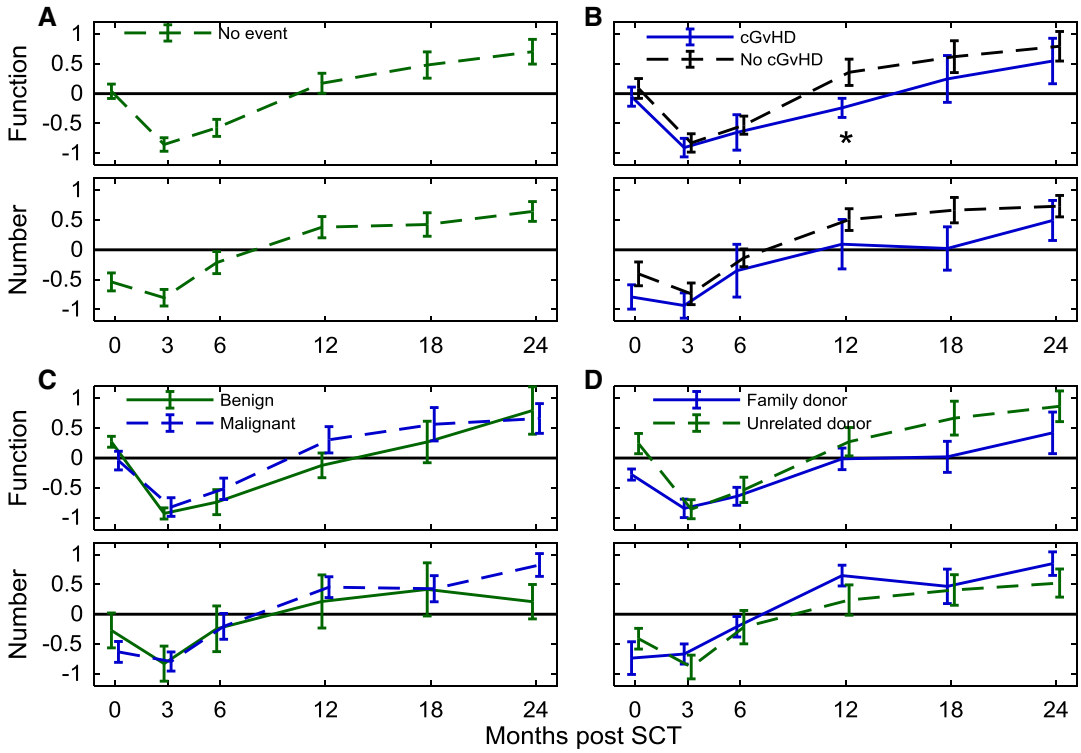

Figure 3. Mean reconstitution curves over time for different subgroups of patients, with error bars showing the standard error of the mean (SEM). Time plots of "function of cells" and "number of cells" were computed with 7 immune variables. (A) Reconstitution curve for patients without events. (B) Reconstitution curves for patients with cGVHD (blue) and without cGVHD (black). (C) Reconstitution curves for patients undergoing HSCT for nonmalignant disease (green) and for malignant disease (blue). (D) Reconstitution curves for patients receiving a graft from an unrelated donor (green) and a from a family donor (blue). Significant differences ($P < .05$) between the 2 subgroups in (B), (C), and (D) were tested at each time point. In (B), a significant difference in immune reconstitution between patients with GVHD and those without GVHD was found at 12 months (P = .039), indicated by a asterisk (*).

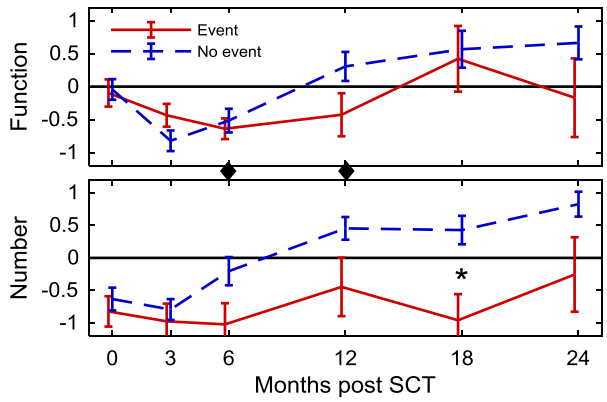

Figure 4. Reconstitution curves for patients with malignant disease only. Red lines show the predicted reconstitution pattern for patients with a subsequent event (censored at the time of the event), and blue lines show the modeled curve for patients who did not experience any event. Significant differences ($P < .05$) between the 2 groups are indicated for "number of cells" and "function of cells" by a asterisk (*), and for ReflComp1= ("number of cells" + "function of cells")/$2^{1/2}$ by a diamond (◆). Significant differences between the 2 groups of patients were found for "number of cells" at 18 months ($P = .049$), indicated by a asterisk (*), and for ReflComp1 = ("number of cells" + "function of cells")/$2^{1/2}$ at 6 months ($P = .024$) and at 12 months ($P = .001$) indicated by a diamond (◆).

characterizing immune reconstitution after HSCT is valuable for the simultaneous interpretation of different parameters at multiple time points to describe the pattern of immune reconstitution in detail. We found that 7 variables were sufficient for constructing a model that is clearly superior to those developed using univariate statistics. The use of single factors at specific time points for predicting patients at risk is tempting in clinical practice, but a more elaborate statistical model is needed to understand the interactions between different variables that are important for the reconstitution of immune function in patients after HSCT.

ACKNOWLEDGMENTS

Financial disclosure: This work was supported by grants from the Swedish Childhood Cancer Fund.

Conflict of interest statement: There are no conflicts of interest to report.

SUPPLEMENTARY MATERIALS

Supplementary material associated with this article can be found in the online version at doi:10.1016/j.bbmt.2019.06.018.

REFERENCES

1. Storek J, Geddes M, Khan F, et al. Reconstitution of the immune system after hematopoietic stem cell transplantation in humans. *Semin Immunopathol*. 2008;30:425–437.
2. Storek J, Gooley T, Witherspoon RP, Sullivan KM, Storb R. Infectious morbidity in long-term survivors of allogeneic marrow transplantation is associated with low CD4 T cell counts. *Am J Hematol*. 1997;54:131–138.
3. Brown JA, Stevenson K, Kim HT, et al. Clearance of CMV viremia and survival after double umbilical cord blood transplantation in adults depends on reconstitution of thymopoiesis. *Blood*. 2010;115:4111–4119.
4. Kim DH, Sohn SK, Won DI, Lee NY, Suh JS, Lee KB. Rapid helper T-cell recovery above 200 × 10^6/L at 3 months correlates to successful transplant outcomes after allogeneic stem cell transplantation. *Bone Marrow Transplant*. 2006;37:1119–1128.
5. Bartelink IH, Belitser SV, Knibbe CA, et al. Immune reconstitution kinetics as an early predictor for mortality using various hematopoietic stem cell sources in children. *Biol Blood Marrow Transplant*. 2013;19:305–313.

6. Berger M, Figari O, Bruno B, et al. Lymphocyte subsets recovery following allogeneic bone marrow transplantation (BMT): $CD4^+$ cell count and transplant-related mortality. *Bone Marrow Transplant*. 2008;41:55–62.
7. Corre E, Carmagnat M, Busson M, et al. Long-term immune deficiency after allogeneic stem cell transplantation: B-cell deficiency is associated with late infections. *Haematologica*. 2010;95:1025–1029.
8. Ogonek J, Kralj Juric M, Ghimire S, et al. Immune reconstitution after allogeneic hematopoietic stem cell transplantation. *Front Immunol*. 2016;7:507.
9. Bayraktar UD, Milton DR, Guindani M, et al. Optimal threshold and time of absolute lymphocyte count assessment for outcome prediction after bone marrow transplantation. *Biol Blood Marrow Transplant*. 2016;22:505–513.
10. Koehl U, Bochennek K, Zimmermann SY, et al. Immune recovery in children undergoing allogeneic stem cell transplantation: absolute $CD8^+$ $CD3^+$ count reconstitution is associated with survival. *Bone Marrow Transplant*. 2007;39:269–278.
11. Ishaqi MK, Afzal S, Dupuis A, Doyle J, Gassas A. Early lymphocyte recovery post-allogeneic hematopoietic stem cell transplantation is associated with significant graft-versus-leukemia effect without increase in graft-versus-host disease in pediatric acute lymphoblastic leukemia. *Bone Marrow Transplant*. 2008;41:245–252.
12. Yakoub-Agha I, Saule P, Magro L, et al. Immune reconstitution following myeloablative allogeneic hematopoietic stem cell transplantation: the impact of expanding $CD28^-$ $CD8^+$ T cells on relapse. *Biol Blood Marrow Transplant*. 2009;15:496–504.
13. Drylewicz J, Schellens IM, Gaiser R, et al. Rapid reconstitution of CD4 T cells and NK cells protects against CMV reactivation after allogeneic stem cell transplantation. *J Transl Med*. 2016;14:230.
14. Gianelli R, Bulleri M, Menconi M, et al. Reconstitution rate of absolute $CD8^+$ T lymphocyte counts affects overall survival after pediatric allogeneic hematopoietic stem cell transplantation. *J Pediatr Hematol Oncol*. 2012;34:29–34.
15. Bemark M, Friskopp L, Saghafian-Hedengren S, et al. A glycosylation-dependent CD45RB epitope defines previously unacknowledged $CD27^-$IgM(high) B cell subpopulations enriched in young children and after hematopoietic stem cell transplantation. *Clin Immunol*. 2013;149:421–431.
16. Forcina A, Noviello M, Carbone MR, Bonini C, Bondanza A. Predicting the clinical outcome of allogeneic hematopoietic stem cell transplantation: the long and winding road toward validated immune biomarkers. *Front Immunol*. 2013;4:71.
17. Skert C, Perucca S, Chiarini M, et al. Sequential monitoring of lymphocyte subsets and of T- and B-cell neogenesis indexes to identify time-varying immunologic profiles in relation to graft-versus-host disease and relapse after allogeneic stem cell transplantation. *PLoS One*. 2017;12: e0175337.
18. Koenig M, Huenecke S, Salzmann-Manrique E, et al. Multivariate analyses of immune reconstitution in children after allo-SCT: risk-estimation based on age-matched leukocyte sub-populations. *Bone Marrow Transplant*. 2010;45:613–621.
19. Ek T, Josefson M, Abrahamsson J. Multivariate analysis of the relation between immune dysfunction and treatment intensity in children with acute lymphoblastic leukemia. *Pediatr Blood Cancer*. 2011;56:1078–1087.
20. Huenecke S, Behl M, Fadler C, et al. Age-matched lymphocyte subpopulation reference values in childhood and adolescence: application of exponential regression analysis. *Eur J Haematol*. 2008;80:532–539.
21. Nierop AFM. *Multidimensional analysis of grouped variables: an integrated approach [dissertation]*. Leiden, The Netherlands: DSWO Press, Leiden University; 1993.
22. Nierop AFM, Tas AC, van der Greef J. Reflected discriminant analysis. *Chemometr Intell Lab Syst*. 1994;25:249–263.
23. Yong MK, Cameron PU, Slavin MA, et al. Low T-cell responses to mitogen stimulation predicts poor survival in recipients of allogeneic hematopoietic stem cell transplantation. *Front Immunol*. 2017;8:1506.
24. Wasserstein RL, Lazar NA. The ASA statement on p-values: context, process, and purpose. *Am Stat*. 2016;70:129–133.
25. Goodpaster AM, Kennedy MA. Quantification and statistical significance analysis of group separation in NMR-based metabonomics studies. *Chemometr Intell Lab Syst*. 2011;109:162–170.
26. Bohmann EM, Fehn U, Holler B, et al. Altered immune reconstitution of B and T cells precedes the onset of clinical symptoms of chronic graft-versus-host disease and is influenced by the type of onset. *Ann Hematol*. 2017;96:299–310.
27. Park BG, Park CJ, Jang S, et al. Reconstitution of lymphocyte subpopulations after hematopoietic stem cell transplantation: comparison of hematological malignancies and donor types in event-free patients. *Leuk Res*. 2015;39:1334–1341.
28. de Koning C, Admiraal R, Nierkens S, Boelens JJ. Immune reconstitution and outcomes after conditioning with anti-thymocyte-globulin in unrelated cord blood transplantation; the good, the bad, and the ugly. *Stem Cell Investig*. 2017;4:38.
29. Retière C, Willem C, Guillaume T, et al. Impact on early outcomes and immune reconstitution of high-dose post-transplant cyclophosphamide vs anti-thymocyte globulin after reduced intensity conditioning peripheral blood stem cell allogeneic transplantation. *Oncotarget*. 2018;9:11451–11464.
30. Admiraal R, Lindemans CA, van Kesteren C, et al. Excellent T-cell reconstitution and survival depend on low ATG exposure after pediatric cord blood transplantation. *Blood*. 2016;128:2734–2741.